Sensors and Actuators B 221 (2015) 434–442

Contents lists available at ScienceDirect

Sensors and Actuators B: Chemical

journal homepage: www.elsevier.com/locate/snb

Facile synthesis and gas sensing properties of La_2O_3–WO_3 nanofibers

Changhao Feng[a], Chong Wang[a], Pengfei Cheng[b], Xin Li[a], Biao Wang[c], Yehui Guan[a], Jian Ma[a], Hong Zhang[a], Yanfeng Sun[a,*], Peng Sun[a], Jie Zheng[a], Geyu Lu[a,*]

[a] State Key Laboratory on Integrated Optoelectronics, College of Electronic Science and Engineering, Jilin University, 2699 Qianjin Street, Changchun 130012, People's Republic of China
[b] School of Aerospace Science and Technology, Xidian University, 266 Xibeng Street, Xian 710126, People's Republic of China
[c] Changchun Institute Optics, Fine Mechanics and Physics, Chinese Academy Sciences, Changchun 130033, People's Republic of China

ARTICLE INFO

Article history:
Received 10 January 2015
Received in revised form 24 June 2015
Accepted 24 June 2015
Available online 28 June 2015

Keywords:
La_2O_3-doped WO_3 nanofibers
Electrospinning
Hot pressing
Gas sensor

ABSTRACT

A series of La_2O_3-doped WO_3 nanofibers were synthesized by an electrospinning method in this work. The structure composition and morphology of nanofibers were characterized by XRD (X-ray diffraction), field emission scanning electron microscopy (FESEM), selected area electron diffractive (SAED), energy dispersive X-ray spectroscopy (EDX), transmission electron microscopy (TEM) and high-resolution transmission electron microscopy (HRTEM). Sensors based on these nanofibers were fabricated by hot-press on the ceramic plates. The gas sensing properties of the undoped and La_2O_3-doped WO_3 (La^{3+}:W^{6+} =1 mol%, 3 mol% and 5 mol%) nanofibers were tested to various gases. The sensors based on La_2O_3-doped WO_3 nanofibers, in which the molar ratio of La^{3+}:W^{6+} is 3:100, exhibit highest response toward 100 ppm acetone, having a response about 12.7, which is almost 2 times higher than that of sensor based on pure WO_3 nanofibers. These results indicate that the acetone sensors based on the La_2O_3-doped WO_3 nanofibers exhibit fast response and good repeatability characteristics, which are promising for acetone sensors which used by air-quality and environmental monitoring.

1. Introduction

Recently, one dimensional (1D) nanomaterials (fibers, belts, rods, spirals and tubes) have been intensively explored and developed [1–4]. Because of their amazing properties such as large surface area to volume ratio, easy control dimension and superior mechanical performance, the 1D functional nanomaterials offer tremendous impact in the field of optics, lithium ion batteries, solar cells, electronics, gas sensors, and so on [5–7]. Various methods have been developed to fabricate 1D nanostructures, such as laser assisted catalytic growth, metal organic chemical vapor deposition (MOCVD), thermal evaporation and electrospinning [8,9]. Among these methods, electrospinning seems to be one of the most simple, versatile and low-cost methods for producing organic or inorganic nanofibers [8–10]. It provides the ability to produce long continuous fibers with typical diameters ranging from 50 nm up to few micrometers and length up to several centimeters. In the past years, it was mainly applied to pure organic polymer. Recently, functional metal oxides nanofibers, including SnO_2 [2,11–14], α-Fe_2O_3 [15–19], WO_3 [20–23], TiO_2 [24–27] and In_2O_3 [28–31] were prepared by electrospinning and mainly applied in the field of gas sensors. In spite of exciting achievements in fabricating gas sensors based on electrospinning have been obtained, the challenge to improve the sensitivity, repeatability and selectivity still exists for the sensors based on 1D nanostructure.

WO_3 (Tungsten oxide), n-type semiconductor materials with a band gap of 2.5–3.0 eV, is a kind of important technologically materials due to their excellent electronic, chemical and optical properties. WO_3 has been widely considered to be one of the most promising sensor materials for detecting gases like NO_2, NH_3, Cl_2 and H_2S. In order to further improve its performance, many approaches, including increasing the surface to volume ratio, preparing WO_3 with different morphologies [32,33], and using special measurement techniques, have been studied in recent years. What's more, adding transition metal oxides as catalyst also becomes a key point for gas sensing applications. As a consequence of its unique electronic structures, La_2O_3 (Lanthanum oxide), n-type basic rare earth oxide with a band gap of 5.5 eV, has outstanding optical, electrical and magnetic properties [34], it has been widely used as capacitors [35] materials for varistors [36] and catalysts for gas sensors [37,38]. Rare earth oxides are well known to display interesting catalytic properties in the environment

* Corresponding authors.
E-mail addresses: syf@jlu.edu.cn (Y. Sun), lugy@jlu.edu.cn (G. Lu).

http://dx.doi.org/10.1016/j.snb.2015.06.114
0925-4005/

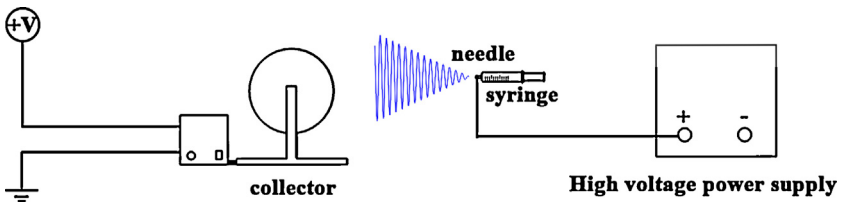

Fig. 1. Schematic illustration of the electrospinning apparatus.

protection, organic synthesis, and synthetic ammonia [50]. Lanthanum oxide (La_2O_3) is the most representative compound among these substances. As already reported, the gas sensing properties will be promoted when SnO_2 or ZnO is loaded with a basic oxide like La_2O_3 [2,39]. Consequently, it has been developed as sensors to detect ethanol, carbon monoxide, carbon dioxide and acetone, etc. For example, B. Bhooloka Rao studied the sensitivity characteristics of La_2O_3–ZnO semi-conductor gas sensors to ethanol vapors [40]. Gopal Reddy et al. presented the gas sensing characteristics of the SnO_2–La_2O_3 system, which detects hydrogen selectively [37]. Kim et al. investigated the gas sensing properties of CO_2 gas sensor, which was fabricated by coating and heat-treating the drop of La solution on the surface of SnO_2 thick film [38]. To the best of our knowledge, there are few reports on the acetone-sensing property of La_2O_3-doped WO_3 nanofibers, which were prepared by electrospinning.

In this work, we developed a facile strategy to prepare a fast response and good repeatability acetone sensor fabricated by hot-pressing La_2O_3-doped WO_3 nanofibers on the ceramic plates. Furthermore, to demonstrate the applications, the gas sensing properties of those nanofibers were investigated. A comparative gas sensing study between the undoped and La_2O_3-doped WO_3 nanofibers was performed. These results indicate that the sensors based on doped nanofibers, in which the molar ratio of La^{3+}:W^{6+} is 3:100, show outstanding sensing properties toward acetone with a quick response and good repeatability characteristics. At last, the effect of La_2O_3-doping was investigated and a possible mechanism is proposed.

2. Experimental

2.1. Synthesis and characterization of La_2O_3-doped WO_3 nanofibers

All the chemical reagents in the experiment were of analytical grade and used as received without further purification. In a typical experiment, tungsten chloride (WCl_6), polyvinyl pyrrolidone (PVP, Mw = 1,800,000) and *N*,*N*-dimethylformamide (DMF) were purchased from Sinopharm-Aldrich, USA. Lanthanum nitrate hydrate ($La(NO_3)_3{\cdot}6H_2O$), acetic acid (CH_3COOH) and absolute ethanol (C_2H_5OH) were purchased from Beijing Chemicals Co., Ltd.

A series of 0, 1, 3 and 5 mol% La_2O_3-doped WO_3 nanofibers (the molar percentage was defined as the ratio of the mole numbers of La^{3+} to that of W^{6+}) were synthesized by electrospinning, labeled as S1, S2, S3 and S4, respectively. In a typical synthesis process, 2 mmol WCl_6 and a certain amount of $La(NO_3)_3{\cdot}6H_2O$ were dissolved in 5 g DMF, 5 g C_2H_5OH and 0.5 g CH_3COOH by magnetic stirring for 1 h at room temperature. Then PVP was added to the above solutions and under stirring for 12 h at 50 °C, until a viscous precursor solution completely was formed. The concentration of PVP in the solution was fixed to be 10 wt% to produce uniform nanofibers. In the process, PVP improves the viscosity of the solution for electrospinning. After fully stirring, the solution was transferred into the syringe attached with a spinneret whose inner diameter is 1.64 mm.

As shown in Fig. 1, the basic setup for electrospinning consists three major components: a collector, a spinneret (a metallic needle) and a high voltage power supply. The relevant parameters were as follows: the voltage and distance between the needle (positive pole) and the collector (negative pole) were 12 kV and 10 cm. The feeding rate of the solution was fixed at 0.3 mL/h by using a syringe pump. The PVP/WCl_6/$La(NO_3)_3$ precursors composite nanofibers were deposited on the collector during the electrospinning procedure. With the aim of decomposing PVP completely, the as-synthesized nanofibers were calcined at 500 °C for 3 h in air, and a moderate heating ratio (2 °C/min) was chosen to remove organic compounds sufficiently.

The X-ray diffraction (XRD) patterns were recorded by a Rigaku TTRIII X-ray diffractometer with Cu-Kα1 radiation ($\lambda = 0.15406$ nm) in the range of 20–60° (2θ) at room temperature. Field emission scanning electron microscopy (FESEM) images were obtained using a JEOL JSM-7500F microscope with an acceleration voltage of 15 kV. The energy-dispersive X-ray spectroscopy (EDX) spots pattern scanning analysis was performed by the TEM attachment. Transmission electron microscopic (TEM) and high-resolution transmission electron microscopic (HRTEM) images, and selected area electron diffractive (SAED) patterns were obtained on a JEOL JEM-3010 transmission electron microscope with an acceleration voltage of 200 kV.

2.2. Fabrication and measurement of gas sensor

Fig. 2(a) and (b) shows photographs of the electrode in the front and back, and Fig. 2(c) shows the schematic image of the blank sensor coated with the sensing material. We hot-pressed the La_2O_3-doped WO_3 nanofibers on ceramic plates (1.0 mm × 1.5 mm), which

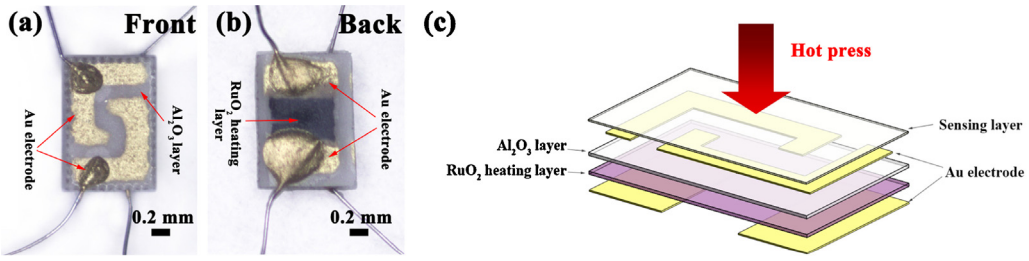

Fig. 2. (a) Photograph of the electrode in the front. (b) Photograph of the electrode in the back. (c) A schematic illustration of the blank sensor coated with the sensing material.

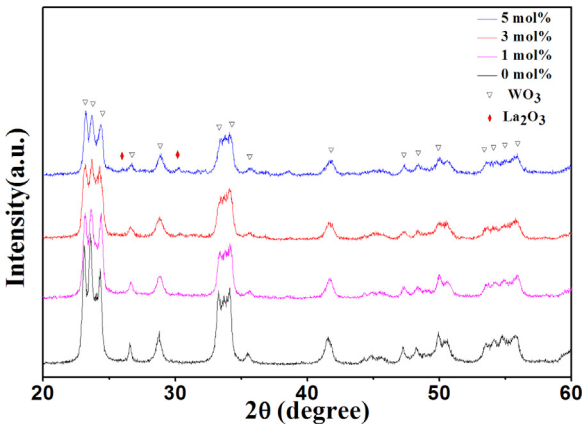

Fig. 3. XRD patterns of La_2O_3–WO_3 nanofibers with different molar ratios.

were coated with two L gold electrodes and ruthenium oxides as heater on the front and back sides by screen printing technique. The calcined nanofibers were mild pressed on the ceramic plates by Hot Press Machine (HS-XX40) with a moderate pressure at 200 °C for 5 min. With the mild heating and pressuring, the materials have a good adhesion to the substrate. The hot-pressed mats did not peel of the substrates during subsequent fabrication processes and made good electrical contact to the electrodes. This process would help stabilizing the microstructure and possibly pre-aging the sensing materials more effectively to achieve improved long-term stability of the sensors. Following the hot-pressing step the samples were calcined at 400 °C for 2 h in air. The morphology of the nanofibers was maintained after the hot-pressing and calcination steps as shown in the SEM images in Fig. 4(e) and (f). The gas-sensing properties of the sensors based on La_2O_3-doped WO_3 nanofibers were evaluated with an Intelligent Test Meter (RQ-2, China). The gas-sensing properties of sensors were measured with a static gas-sensing characterization system, as diagrammed in our previous works [8,32]: first, fresh air (atmospheric air) was introduced into a closed glass chamber, and then a given amount of the tested gas was injected into the chamber by a micro-injector, finally the sensor was put into the chamber for the measurement of the response performance. The desired concentration of the volatile organic compounds (VOC) was obtained by the static liquid gas distribution method [41], which was calculated by formula (1):

$$C = \frac{22.4 \times \varphi \times \rho \times V_1}{M \times V_2} \quad (1)$$

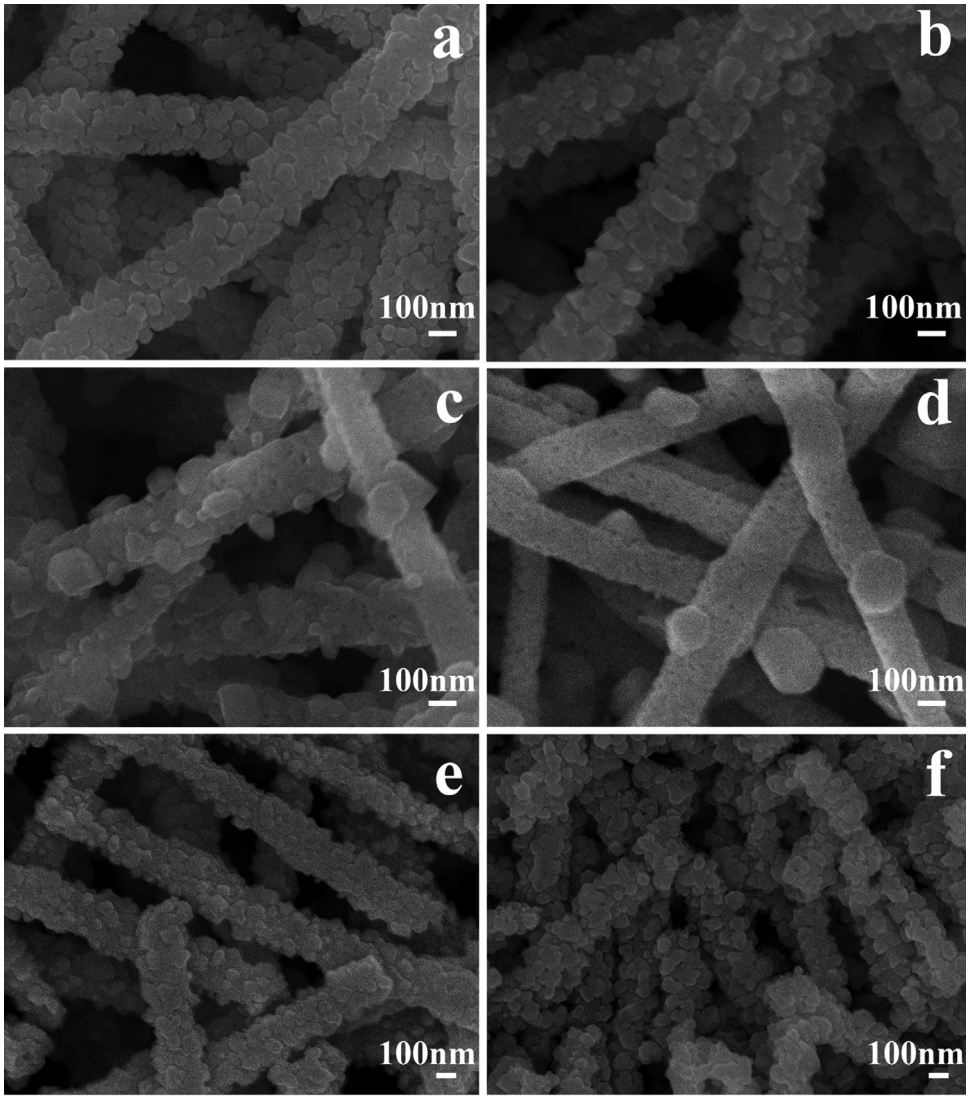

Fig. 4. FESEM images of (a) S1, (b) S2, (c) S3, (d) S4, (e) and (f) are S1 nanofibers before and after hot press.

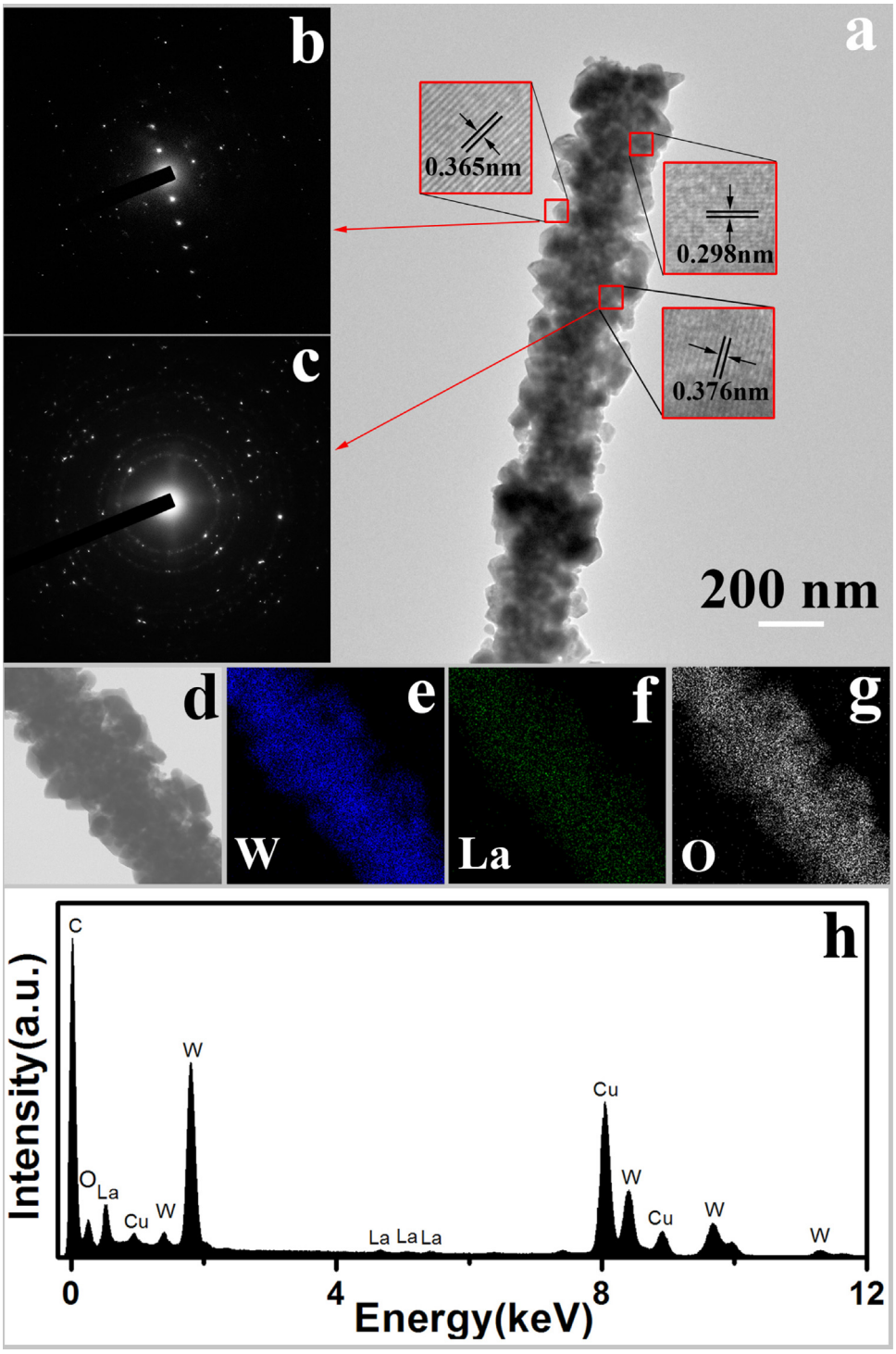

Fig. 5. (a) TEM and HRTEM images pattern of the S3 nanofibers. (b) and (c) are selected area electron diffraction (SAED) patterns. (d)-(g) are EDX elemental maps and (g) spots pattern of W, La and O respectively.

where C (ppm) is the target gas concentration, φ the required gas volume fraction, ρ (g/mL) the density of the liquid, V_1 (μL) the volume of liquid, V_2 (L) the volume of the chamber and M (g/mol) the molecular weight of the liquid. The gas-sensing properties of sensors were tested under the condition (RH: 20–30%; temperature: 20–25 °C). The gas response was defined as R_a/R_g, where R_a and R_g are the resistances in air and tested gas atmosphere, respectively. The response and recovery times were defined as the time taken by sensors to achieve 90% of the total resistance change in the case of adsorption and desorption, respectively [42].

3. Results and discussion

Fig. 3 shows typical XRD patterns of the synthesized nanofibers. As shown in Fig. 3, the crystal phase of material S1 is WO_3, and the diffraction peaks can be readily indexed to (0 0 2), (0 2 0) and (2 0 0) reflections of a monoclinic WO_3 phase, which is agreed well with the reported values from the Joint Committee on Powder Diffraction Standards card (JCPDS card No. 83-950). With the increment of the La_2O_3-doping amount, the diffraction peaks of 26.09° and 29.97°, which is indexed to (1 1 0) and (1 0 1) crystal planes of La_2O_3

(JCPDS card No. 74-2430), become much stronger and sharper. Such results demonstrate that the products of S2, S3 and S4 are composite oxides of WO_3 and La_2O_3. No other diffraction peaks are observed, indicating the absence of other impurities.

The morphologies of the synthesized nanofibers were observed by using FESEM, and all the nanofibers have a uniform diameter about 200 nm as shown in Fig. 4. The FESEM images of S1 (pure WO_3) nanofibers after calcined is shown in Fig. 4a, from which a number of nanofibers composed by many nanoparticles can be clearly observed. No other morphologies can be detected from the FESEM image of WO_3 nanofibers, indicating a high yield of these nanostructures. Fig. 4(b)–(d) show the FESEM images of La_2O_3–WO_3 nanofibers samples (S2–S4). It can be observed that the morphologies of those nanofibers have changed obviously compared with S1. Those nanofibers are composed by backbones, which are constructed by small crystal grains, and some big nanoparticles decorated on those backbones. The nanoparticles which were decorated on backbones are monocrystalline, that is proved later by the results of SAED (as shown in Fig. 5(b)). However, with the increment of doping amount, the grain size which composed the backbone in S3 (as shown in Fig. 4(c)) is smaller than that in S2 (as shown in Fig. 4(b)) obviously, and the grain boundary of S4 can hardly be observed. And the decrease of grains size indicates that the La_2O_3 doping impedes the growth of WO_3. This is likely because that the La^{3+} ions (0.105 nm) are considerably larger than W^{6+} ions (0.058 nm) [49], which is also proved by Yamazoe in his work [43]. Fig. 4e and 4f show the FESEM images of S1 nanofibers before and after hot-press, demonstrating that after hot-press the nanofibers significantly became short but the morphology of nanofibers are not change obviously.

To further study the internal structure of the nanofibers, transmission electron microscopy (TEM) combined with high-resolution transmission electron microscopy (HRTEM), selected area electron diffraction (SAED) analysis techniques and energy dispersive X-ray spectroscopy (EDX) were employed. The typical TEM image of S3 (La^{3+}/W^{6+} = 3 mol%) nanofibers (Fig. 5a) show that the size and morphologies are similar to the results of FESEM. The insets show the HRTEM images which obtained from the marked circles in Fig. 5a. The lattice fringes could be clearly observed and the lattice spacings are 0.365 nm and 0.376 nm, corresponding to the (2 0 0) and (0 2 0) plane of WO_3, respectively. The lattice spacing is 0.298 nm, which is corresponding to the (0 1 1) plane of La_2O_3. Fig. 5b shows a SAED pattern from the marked circle of the big particle which decorated on the backbones, and it proves that those particles are monocrystalline in nature. Fig. 5c is the SAED pattern from the marked circle in backbone, which demonstrates that the backbones of those nanofibers are polycrystalline in nature. EDX elemental mapping was conducted to clearly identify the spatial distribution of W, O and La in the nanofibers structure (Fig. 5(d)–(g)). And the peaks of W, O and La could be clearly seen in Fig. 5 h. What's more, the real ratio of La^{3+} to W^{6+} in S3 nanofibers is 2.64:100, which is performed by energy-dispersive X-ray spectroscopy (EDX). Therefore, it clearly shows that the nanofibers densely consist of WO_3 and La_2O_3 nanoparticles.

As one of highly volatile organic compounds, acetone is widely used as an organic solvent (plastic, fiber and spray-paint) or chemicals intermediate (dyestuff, rubber, and lubricating oil). Although it is popularly regarded as relatively low toxic, some investigations have indicated that chronically exposure may damage to the liver, kidney and nerve. Compared with the various traditional analytical systems, gas sensors have been acknowledged as simple and inexpensive tools for detection and quantification of toxic pollutant gases, combustible gases and organic vapors [44]. Acetone gas sensors are in great demand due to the growing concern about air-quality and environmental monitoring. Therefore, to demonstrate the potential application, gas sensors based on S1, S2, S3 and S4 nanofibers were fabricated and their gas sensing performances were investigated. It is well known that the response of a gas sensor is highly influenced by its operating temperature. In order to determine the optimum operating temperature, the response of sensors based on S1, S2, S3 and S4 nanofibers to 100 ppm acetone were tested as a function of operating temperature as shown in Fig. 6. It is obvious that the responses of these sensors varied from 275 °C to 400 °C. Each sensor had an optimal operating temperature, at which the sensors exhibited the highest response to acetone gas. It can be seen that the gas sensor based on S1 nanofibers has a maximum gas response at 300 °C, while the sensors based on the S2 and S4 nanofibers have the maximum gas response at 325°C and 375 °C, respectively. For S3 gas sensors, it is clearly seen that with temperature increasing, the responses rise monotonically in the range of 275–350 °C, and reach the maximum value at 350 °C, and decrease with a further increase of the operating temperature. Among these sensors, the sensors based on S3 nanofibers showed the highest response toward 100 ppm acetone, with the maximum response of 12.7. The response of sensors which based on S3 nanofibers was about 2 times higher than sensors based on S1 nanofibers.

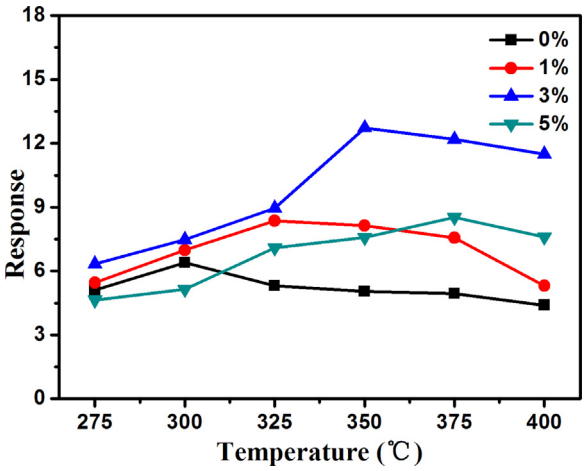

Fig. 6. Response of sensors based on S1, S2, S3 and S4 nanofibers to 100 ppm acetone as function of the operating temperature.

It is well known that reducing gases react most effectively with chemisorbed oxygen on metal oxides semiconductor optimally at a particular temperature, which made the resistance decrease significantly in acetone gas [45]. For sensors S3, there is not enough energy to make full reaction between oxygen species and acetone vapor when the temperature below 350 °C. While at temperature 350 °C, all the oxygen species may have the required energy to react with acetone molecules. But when the temperatures above 350 °C, the amount of oxygen ion species adsorbed on the surface sites of the nanofibers may be insufficient to react with acetone molecules, and more electrons would jump into the conductions band at higher temperatures, so the resistance in air (R_a) and the response ($R = R_a/R_g$) will decrease. Therefore, 350 °C was selected as the operating temperature for sensor based on S3 nanofibers in the following gas testing process.

Gas response of sensors based on S1 and S3 nanofibers upon exposures to different concentrations of acetone ranging from 0.8 to 200 ppm at the optimum operating temperature is displayed in Fig. 7. From the two curves, it is found that the response of sensors increased with the gas concentrations. The response of sensors based on S3 nanofibers is 17.8 for 200 ppm acetone vapor, and the detection limit of this sensor is 0.8 ppm with a response of 1.8; the response of sensors S1 is 10.1 for 200 ppm acetone. And the detection limit is 1 ppm with a response of 1.2. Moreover, the responses were proportional to the increasing concentrations of

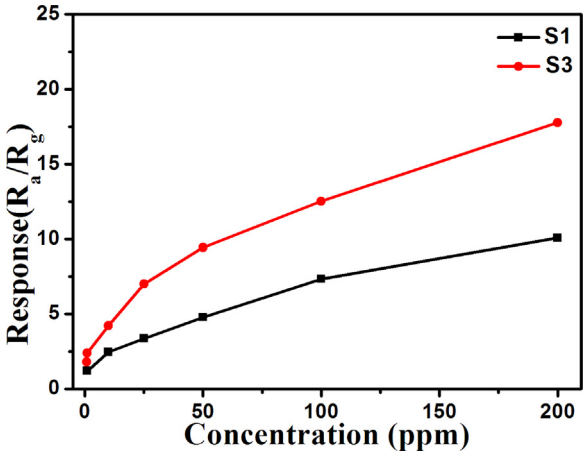

Fig. 7. Response of sensors based on S1 and S3 nanofibers toward acetone at different concentrations.

acetone, when the gas concentrations were corresponding low. What's more, the response to acetone for the sensors S3 is obviously higher than that of S1. It can be concluded that the doping of La_2O_3, especially with the La_2O_3/WO_3 = 3 mol%, has a great influence on the sensing prosperities.

Then, the dynamic response characteristics of sensors based on the S3 nanofibers to acetone vapors were investigated. It can be seen that sensors showed sensitive and reversible response to acetone as shown in Fig. 8(a) and (b). Fig. 8(a) shows the dynamic response of sensors based on S3 nanofibers to 50 ppm acetone, it

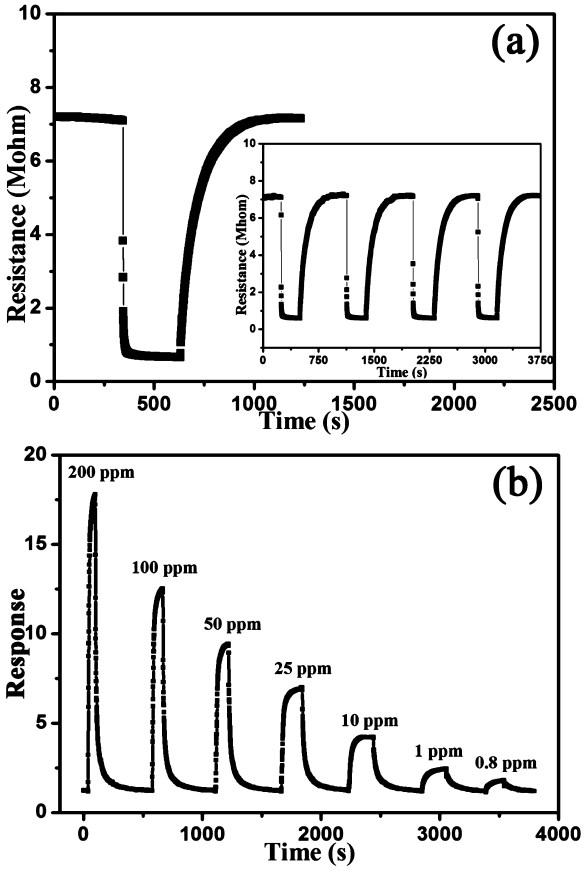

Fig. 8. (a) The dynamic response of the sensor based on S3 nanofibers to 50 ppm acetone. (b) The response and recovery curves of the gas sensor S3 to different concentrations of acetone at the operating temperature.

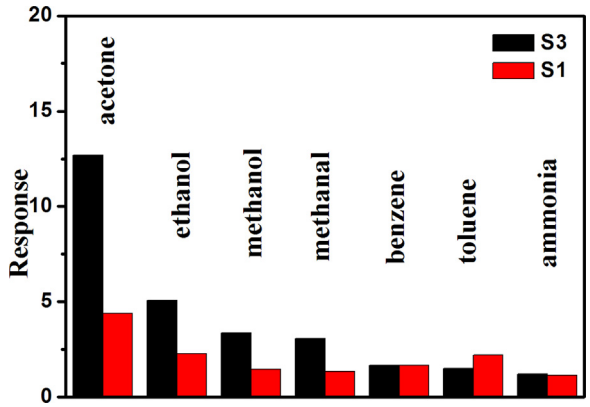

Fig. 9. Comparison in sensor S1 and S3 response to different gas with a same concentration.

presents a fast response and recovery process, and the response and recovery time are about 6 s and 210 s, corresponding to achieve 90% of the total resistance change in the case of adsorption and desorption, respectively. The four reversible cycles of the response curve indicates the repeatable characteristics of sensors S3, as shown in the inset of Fig. 8(a). It is noted that sensors fabricated in our work exhibits good sensing performances. Fig. 8(b) shows the response and recovery curves of gas sensors S3 upon being orderly exposed to different concentrations of acetone at the operating temperature. It is clear that the response and recovery characteristics were almost reproducible as well as the quick response and recovery times. When sensors S3 were exposed to 200 ppm acetone, the response was 17.8. With decreasing the concentration of acetone, the responses decreased. The responses were about 17.8, 12.5, 9.4, 7.0, 4.2, 2.4 and 1.8 to 200, 100, 50, 25, 10, 1 and 0.8 ppm acetone, respectively. It was worth noting that these sensors had good repeatability and stability prosperities.

As we all know, through doping La_2O_3 into n-type sensing materials (SnO_2, ZnO and WO_3), both the selectivity and responses of sensors to acetone and ethanol gas can be improved [46,49,51]. Fig. 9 shows the response of sensors S1 and S3 in low RH air (25%) to 100 ppm different test gases at the operating temperature. Seven kinds of gases were tested, including acetone, ethanol, methanol, methanol, benzene, toluene and ammonia. It can be seen that sensors based on S1 nanofibers exhibited a response to acetone, ethanol and toluene, and less effective response to any other test gases. And sensors based on S3 nanofibers displayed enhanced response to acetone, ethanol, methanol and methanal by compare with that based on S1 nanofibers. However, by comparing the sensing behavior to various test gases, sensors based on S3 nanofibers exhibit the highest response to acetone among the tested gas, and the response to 100 ppm acetone vapor is about 12.7, while the responses to other gases are below 5.1. Consequently, it is concluded that sensor S3 showed selectivity toward acetone opposed to the detected other gases at the same concentrations.

From the view of the practical applications, in order to ensure the accuracy of detection, gas sensors should maintain good long-term stability. Therefore, the experiment on the long term stability of sensor S3 to 100 ppm acetone was carried out under the optimum conditions over 30 days, as displayed in Fig. 10. As the nanofibers contain many grain boundaries, the response degraded a little for long term measurement, the transient sensing responses of S3 in day 1, 5, 10, 15, 20, 25 and 30 are shown in the Fig. S1. After 30 days, the response of sensor S3 degrade from 12.7 to 10.5. Hence, a good stability of the sensors based on La_2O_3 doped WO_3 nanofibers is obtained. With these good gas sensing feature, the present sensor bade on La_2O_3 doped WO_3 nanofibers might to be a promising practical sensor.

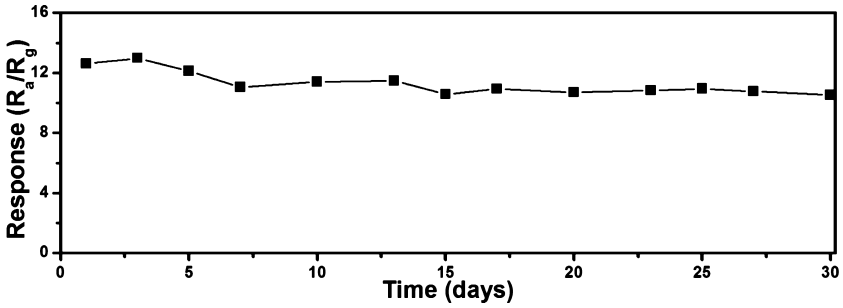

Fig. 10. Long-term stability of sensor S3 at the operating temperature.

The acetone gas sensing mechanisms of n-type metal oxides are closely related to the change of resistances, which are controlled by the reaction of test gas molecules and the chemisorbed oxygen on the surface. When the sensors are exposed to air, the adsorbed oxygen species can obtain free electrons from the conduction band of La_2O_3 and WO_3, resulting into the formation of ionic species such as O^- or O_2^- [20]. The electrons transfer from the conduction band to the chemisorbed oxygen result in the decrease of the electron concentration in the sensing materials. The decreasing of carrier concentration and electron mobility are result in the rise of resistance. Oxygen is ionsorbed predominantly as O^- ions, when the temperature is in range of 420–670 K [20], which is the general operating temperature range, as shown in Eqs. (2)–(4)

$$O_{2(gas)} \leftrightarrow O_{2(adsorbed)} \quad (2)$$

$$O_{2(absorbed)} + e^- \leftrightarrow O_2^- \quad (3)$$

$$O_2^- + e^- \leftrightarrow 2O^- \quad (4)$$

On the contrary, when the sensors are exposed to acetone vapors, the ionic oxygen species adsorbed on the surface of sensing materials will react with acetone molecules. The reaction of acetone vapor with chemisorbed oxygen is explained by Kim et al. [21] as follows:

$$CH_3COCH_{3(gas)} + O^- \rightarrow CH_3COC^+H_2 + OH^- + e^- \quad (5)$$

$$CH_3COCH_{3(gas)} + 2O^- \rightarrow C^+H_3 + CO_2 + CH_3O^- + 2e^- \quad (6)$$

This process will release the trapped electrons back to the conductance of La_2O_3 and WO_3, and inducing an increase in electron concentration, and that would decrease the resistance of the sensor. What's more, the addition of La_2O_3 was essential for WO_3 to promote the acetone sensing properties. The basic character of the La_2O_3 modified WO_3 surface, involves a stabilization of the surface oxygen species with negative charge (e.g., O^{2-}) [37]. And the catalytic activity of La_2O_3 devotes to increase the response to acetone, since the addition of La_2O_3 would brought about enhancement of catalytic activity not only for the dehydrogenation but also accelerate consecutive oxidation of hydrocarbons [39,46]. And the dehydrogenation process is more probable on the surface with basic property. And La_2O_3 as a basic metal oxide additive has markedly promoted the response to acetone vapor. This is also the reason why the responses of sensors S3 to ethanol, methanol and methanal are improved a little at the same time. Therefore, the gas sensors based on S3 and S4 nanofibers exhibit better acetone response than S1 and S2. What's more, the diameter of grain which composed of S1 nanofibers is ~55 nm; the grain size of S2 nanofibers is ~26 nm, while the grain boundaries of S4 are hardly be observed, as shown in Fig. 4. This is because the excess of La_2O_3 acting as a grain growth inhibitor not allowing the crystallite size to increase even at higher sintering temperatures, which was also confirmed by Yamazoe in their studies [43]. According to Li et al. [47] and Hyodo et al. [48], grain boundaries or grain junctions are considered as the active sites and they act positively on the sensor response. However, grain boundaries on the surface of the S4 nanofibers are unobvious compared with that of S3 nanofibers. For this reason, the response of sensor based on S4 nanofibers is lower than sensors based on S3 nanofibers. Further study and systematic experiments are needed for the deep understanding of the La_2O_3–WO_3 nanofibers induced sensing properties.

4. Conclusion

In summary, a series of La_2O_3–WO_3 nanofibers have been synthesized through a simple and facile electrospinning technique. The results of characterization indicate that nanofibers with La^{3+}/W^{6+} = 3 mol% demonstrate significantly enhanced response to acetone compared with other counterpart. The gas sensor based on S3 nanofibers demonstrated good selectivity and repeatability at the optimum temperature. The La_2O_3 worked most effectively as a catalyst not only for the dehydrogenation but also accelerate consecutive oxidation of hydrocarbons. The good acetone-sensing characteristic indicates that the present sensors based on La_2O_3–WO_3 nanofibers are promising for acetone sensors which used by air-quality and environmental monitoring.

Acknowledgements

This work is supported by Application and Basic Research of Jilin Province (20130102010JC), the National Nature Science Foundation of China (Nos. 61134010, 61304242, 61327804, 61377058 and 61374218), Program for Chang Jiang Scholars and Innovative Research Team in University (No. IRT13018), Development Program of China (863 Program, Nos. 2013AA030902 and 2014AA06A505), the Project Development Plan of Science and Technology of Jilin Province (20130521009JH), the Fundamental Research Funds for the Central Universities (Nos. JB151304 and XJS14070) and National High-Tech Research and China Scholarship Council.

Appendix A. Supplementary data

Supplementary data associated with this article can be found, in the online version, at http://dx.doi.org/10.1016/j.snb.2015.06.114

References

[1] R.A. Kadir, Z. Li, A.Z. Sadek, R.A. Rani, A.S. Zoolfakar, M.R. Field, J.Z. Ou, A.F. Chrimes, K. Kalantar-zadeh, Electrospun granular hollow SnO_2 nanofibers hydrogen gas sensors operating at low temperatures, J. Phys. Chem. C 118 (2014) 3129–3139.
[2] I.S. Hwang, J.K. Choi, H.S. Woo, S.J. Kim, S.Y. Jung, T.Y. Seong, I.D. Kim, J.H. Lee, Facile control of C_2H_5OH sensing characteristics by decorating discrete Ag nanoclusters on SnO_2 nanowire networks, Appl. Mater. Interfaces 3 (2011) 3140–3145.
[3] S. Xu, Y. Shi, Low temperature high sensor response nano gas sensor using ITO nanofibers, Sens. Actuators B 143 (2009) 71–75.

[4] C.L. Zhang, S.H. Yu, Nanoparticles meet electrospinning: recent advances and future prospects, Chem. Soc. Rev. 43 (2014) 4423–4448.
[5] C. Gao, X. Li, B. Lu, L. Chen, Y. Wang, F. Teng, J. Wang, Z. Zhang, X. Pan, E. Xie, A facile method to prepare SnO_2 nanotubes for use in efficient SnO_2–TiO_2 core-shell dye-sensitized solar cells, Nanoscale 4 (2012) 3475–3481.
[6] S.H. Ahn, D.J. Kim, W.S. Chi, J.H. Kim, One-dimensional hierarchical nanostructures of TiO_2 nanosheets on SnO_2 nanotubes for high efficiency solid-state dye-sensitized solar cells, Adv. Mater. 25 (2015) 4893–4897.
[7] W. Tian, T. Zhai, C. Zhang, S. Li, X. Wang, F. Liu, D. Liu, X. Cai, K. Tsukagoshi, D. Golberg, Y. Bando, Low-cost fully transparent ultraviolet photodetectors based on electrospun ZnO–SnO_2 heterojunction nanofibers, Adv. Mater. 25 (2013) 4625–4630.
[8] D. Li, Y.N. Xia, Fabrication of titania nanofibers by electrospinning, Nano Lett. 3 (2003) 555–560.
[9] C. Feng, X. Li, J. Ma, Y. Sun, C. Wang, P. Sun, J. Zheng, Geyu Lu, Facile synthesis and gas sensing properties of In_2O_3–WO_3 heterojunction nanofibers, Sens. Actuators B 209 (2015) 622–629.
[10] D. Li, Y. Xia, Electrospinning of nanofibers: reinventing the wheel? Adv. Mater. 16 (2004) 1151–1170.
[11] Y. Zhang, J. Li, G. An, X. He, Highly porous SnO_2 fibers by electrospinning and oxygen plasma etching and its ethanol-sensing properties, Sens. Actuators B 144 (2010) 43–48.
[12] W. Tang, J. Wang, P. Yao, X. Li, Hollow hierarchical SnO_2–ZnO composite nanofibers with heterostructure based on electrospinning method for detecting methanol, Sens. Actuators B 192 (2014) 543–549.
[13] Y. Zhang, X. He, J. Lia, Z. Miao, F. Huang, Fabrication and ethanol-sensing properties of micro gas sensor based on electrospun SnO_2 nanofibers, Sens. Actuators B 132 (2008) 67–73.
[14] Q. Qi, T. Zhang, L. Liu, X. Zheng, G. Lu, Improved NH_3,C_2H_5OH, and CH_3COCH_3 sensing properties of SnO_2 nanofibers by adding block copolymer P123, Sens. Actuators B 141 (2009) 174–178.
[15] H. Fan, T. Zhang, X. Xu, N. Lv, Fabrication of N-type Fe_2O_3 and P-type $LaFeO_3$ nanobelts by electrospinning and determination of gas-sensing properties, Sens. Actuators B 153 (2011) 83–88.
[16] Y. Wang, J. Cao, S. Wang, X. Guo, J. Zhang, H. Xia, S. Zhang, S. Wu, Facile synthesis of porous α-Fe_2O_3 nanorods and their application in ethanol sensors, J. Phys. Chem. C 112 (2008) 17804–17808.
[17] C.L. Zhu, H.L. Yu, Y. Zhang, T.S. Wang, Q.Y. Ouyang, L.H. Qi, Y.J. Chen, X.Y. Xue, Fe_2O_3/TiO_2 tube-like nanostructures: synthesis, structural transformation and the enhanced sensing properties, ACS Appl. Mater. Interfaces 4 (2012) 665–671.
[18] H. Shan, C. Liu, L. Liu, S. Lia, L. Wang, X. Zhang, Xi. Bo, X. Chi, Highly sensitive acetone sensors based on La-doped α-Fe_2O_3 nanotubes, Sens. Actuators B 184 (2013) 243–247.
[19] X. Li, H. Zhang, C. Feng, Y. Sun, J. Ma, C. Wang, G. Lu, Novel cage-like α-Fe_2O_3/SnO_2 composite nanofibers by electrospinning for rapid gas sensing properties, RSC Adv. 4 (2014) 27552–27555.
[20] D. Chen, X. Hou, T. Li, L. Yin, B. Fan, H. Wang, X. Li, H. Xu, H. Lu, R. Zhang, J. Sun, Effects of morphologies on acetone-sensing properties of tungsten trioxide nanocrystals, Sens. Actuators B 153 (2011) 373–381.
[21] S.J. Choi, I. Lee, B.H. Jang, D.Y. Youn, W.H. Ryu, C.O. Park, I.D. Kim, Selective diagnosis of diabetes using Pt-functionalized WO_3 hemitube networks as a sensing layer of acetone in exhaled breath, Anal. Chem. 85 (2013) 1792–1796.
[22] M. D'Arienzo, L. Armelao, C.M. Mari, S. Polizzi, R. Ruffo, R. Scotti, F. Morazzon, Macroporous WO_3 thin films active in NH_3 sensing: role of the hosted Cr isolated centers and Pt nanoclusters, J. Am. Chem. Soc. 133 (2011) 5296–5304.
[23] J. Leng, X. Xu, N. Lv, H. Fan, T. Zhang, Synthesis and gas-sensing characteristics of WO_3 nanofibers via electrospinning, J. Colloid Interface Sci. 356 (2011) 54–57.
[24] I. Kim, A. Rothschild, B.H. Lee, D.Y. Kim, S.M. Jo, H.L. Tuller, Ultrasensitive chemiresistors based on electrospun TiO_2 nanofibers, Nano Lett. 6 (2006) 2009–2013.
[25] J.Y. Park, S.W. Choi, J.W. Lee, C. Lee, S.S. Kim, Synthesis and gas sensing properties of TiO_2–ZnO core-shell nanofibers, J. Am. Ceram. Soc. 92 (2009) 2551–2554.
[26] W. Jia, L. Su, Y. Ding, A. Schempf, Y. Wang, Y. Lei, Pd/TiO_2 nanofibrous membranes and their application in hydrogen sensing, J. Phys. Chem. C 113 (2009) 16402–16407.
[27] J. Moon, J. Park, S. Lee, T. Zyung, I. Kim, Pd-doped TiO_2 nanofiber networks for gas sensor applications, Sens. Actuators B 149 (2010) 301–305.
[28] W. Zheng, X. Lu, W. Wang, Z. Li, H. Zhang, Y. Wang, Z. Wang, C. Wang, A highly sensitive and fast-responding sensor based on electrospun In_2O_3 nanofibers, Sens. Actuators B 142 (2009) 61–65.
[29] L. Xu, B. Dong, Y. Wang, X. Bai, Q. Liu, H. Song, Electrospinning preparation and room temperature gas sensing properties of porous In_2O_3 nanotubes and nanowires, Sens. Actuators B 147 (2010) 531–538.
[30] S.K. Lim, S.H. Hwang, D. Chang, S. Kim, Preparation of mesoporous In_2O_3 nanofibers by electrospinning and their application as a CO gas sensor, Sens. Actuators B 149 (2010) 28–33.
[31] P.S. Khiabani, A. Hosseinmardi, E. Marzbanrad, S. Ghashghaie, C. Zamani, M. Keyanpour-Rad, B. Raissi, NO_2 gas sensor fabrication through AC electrophoretic deposition from electrospun In_2O_3 nanoribbons, Sens. Actuators B 162 (2012) 102–107.
[32] C. Wang, R. Sun, X. Li, Y. Sun, P. Sun, F. Liu, G. Lu, Hierarchical flower-like WO_3 nanostructures and their gas sensing properties, Sens. Actuators B 204 (2014) 224–230.
[33] C. Wang, X. Li, B. Wang, J. Ma, Y. Cao, Y. Sun, G. Lu, One-pot synthesis of cuboid WO_3 crystal and its gas sensing properties, RSC Adv. 4 (2014) 18365–18369.
[34] W. Fan, W. Zhao, L. You, X. Song, W. Zhang, H. Yu, S. Sun, A simple method to synthesize single-crystalline lanthanide orthovanadate nanorods, J. Solid State Chem. 177 (2004) 4399–4403.
[35] G. Mavrou, S. Galata, P. Tsipas, A. Sotiropoulos, Y. Panayiotatos, A. Dimoulas, E.K. Evangelou, J.W. Seo, Ch. Dieker, Electrical properties of La_2O_3 and HfO_2/La_2O_3 gate dielectrics for germanium metal-oxide-semiconductor devices, J. Appl. Phys. 103 (2008) 014506.
[36] M.M. Oliveira, P.R. Bueno, E. Longo, J.A. Varela, Influence of La_2O_3, Pr_2O_3 and CeO_2 on the nonlinear properties of SnO_2 multicomponent varistors, Mater. Chem. Phys. 74 (2002) 150–153.
[37] C.V. Gopal Reddy, S.V. Manorama, Room temperature hydrogen sensor based on SnO_2:La_2O_3, J. Electrochem. Soc. 147 (2000) 390–393.
[38] D.H. Kim, J.Y. Yoon, H.C. Park, K.H. Kim, CO_2-sensing characteristics of SnO_2 thick film by coating lanthanum oxide, Sens. Actuators B 62 (2000) 61–66.
[39] T. Jinkawa, G. Sakai, J. Tamaki, N. Miura, N. Yamazoe, Relationship between ethanol gas sensitivity and surface catalytic property of tin oxide sensors modified with acidic or basic oxides, J. Mol. Catal. A: Chem. 155 (2000) 193–200.
[40] B. Bhooloka Rao, Zinc oxide ceramic semi-conductor gas sensor for ethanol vapour, Mater. Chem. Phys. 64 (2000) 62–65.
[41] P. Sun, X. Zhou, C. Wang, B. Wang, X. Xu, G. Lu, One-step synthesis and gas sensing properties of hierarchical Cd-doped SnO_2 nanostructures, Sens. Actuators B 190 (2014) 32–39.
[42] Y.J. Choi, I.S. Hwang, J.G. Park, K.J. Choi, J.H. Park, J.H. Lee, Novel fabrication of an SnO_2 nanowire gas sensor with high sensitivity, Nanotechnology 19 (2008) 095508.
[43] N. Yamazoe, G. Sakai, K. Shimanoe, Oxide semiconductor gas sensors, Catal. Surv. Asia 7 (2003) 63–75.
[44] X. Zhou, J. Liu, C. Wang, P. Sun, X. Hu, X. Li, K. Shimano, N. Yamazoe, G. Lu, Highly sensitive acetone gas sensor based on porous $ZnFe_2O_4$ nanospheres, Sens. Actuators B 206 (2015) 577–583.
[45] J.H. Lee, Gas sensors using hierarchical and hollow oxide nanostructures: overview, Sens. Actuators B 140 (2009) 319–336.
[46] J.Q. He, J. Yin, D. Liu, L.X. Zhang, F.S. Cai, L.J. Bie, Enhanced acetone gas-sensing performance of La_2O_3-doped flowerlike ZnO structure composed of nanorods, Sens. Actuators B 182 (2013) 170–175.
[47] T. Hyodo, N. Nishida, Y. Shimizu, M. Egashira, Preparation and gas-sensing properties of thermally stable mesoporous SnO_2, Sens. Actuators B 83 (2002) 209–215.
[48] Z. Guo, J.L. Liu, Y. Jia, X. Chen, F. Meng, M. Li, J. Liu, Template synthesis, organic gas-sensing and optical properties of hollow and porous In_2O_3 nanospheres, Nanotechnology 19 (2008) 345704.
[49] S. Luo, G. Fu, H. Chen, Y. Zhang, Gas sensing properties and complex impedance analysis of La_2O_3-added WO_3 nanoparticles to VOC gases, Mater. Chem. Phys. 109 (2008) 541–546.
[50] L. Tang, Y. Li, K. Xu, X. Hou, Y. Lv, Sensitive and selective acetone sensor based on its cataluminescence from nano-La_2O_3 surface, Sens. Actuators B 132 (2008) 243–249.
[51] N.V. Hieu, H.R. Kim, B.K. Ju, J.H. Lee, Enhanced performance of SnO_2 nanowires ethanol sensor by functionalizing with La_2O_3, Sens. Actuators B 133 (2008) 228–234.

Biographies

Changhao Feng received his MS degree from department of electronic sciences and technology, Heilongjiang University, China in 2012. He entered the Ph.D. course in 2013, majored in physical electronics. Now, he is engaged in the synthesis and characterization of the semiconducting functional materials and gas sensors.

Chong Wang received the B. Eng. degree in department of electronic sciences and technology in 2013. Now she is currently studying for her M.E. Sci. degree in College of Electronic Science and Engineering, Jilin University, China.

Pengfei Cheng obtained his Ph.D. from Jilin University of China in 2013. Now, he is engaged in the synthesis and characterization of the semiconducting functional materials and dye-sensitized solar cells.

Xin Li received the B. Eng. degree in department of electronic sciences and technology in 2013. Now he is currently studying for his M.E. Sci. degree in College of Electronic Science and Engineering, Jilin University, China.

Biao Wang obtained his Ph.D. degree from Jilin University, China in 2008. Now he is an associate research professor in Changchun Institute of Optics, Fine Mechanics and Physics, Chinese Academy of Science. His current research is laser gas sensor.

Yehui Guan received the B. Eng. degree in department of electronic science and technology in 2014. He is currently studying for his M.E. Sci. degree in College of ElectronicScience and Engineering, Jilin University, China.

Jian Ma received his MS in 2009 from Jilin University at the Electronics Science and Engineering department. Presently, he is working as Technical Assistant in Electronics Science and Engineering department. His current research interests are gas sensor, the design and fabrication of micro-hot plates.

Hong Zhang obtained her Ph.D. from Jilin University of China in 2008. Presently, she is working as lecturer in Electronics Science and Engineering department of Jilin University. Her current research interests are image processing and sensor technology.

Yanfeng Sun obtained his Ph.D. from Jilin University of China in 2007. Presently, he is working as associate professor in Electronics Science and Engineering department of Jilin University. His current research interests are nanoscience and gas sensors.

Peng Sun received his Ph.D. degree from Jilin University of China in 2014. Now, he is engaged in the synthesis and characterization of the semiconducting functional materials and gas sensors.

Jie Zheng received the B.S. degrees in Physics from Northeast Normal University, Changchun, China, in 1984 and received the Ph.D. degrees in Condensed State Physics from Changchun Institute of Optics, Fine Mechanics and Physics, Chinese Academy of Sciences in 2003, and then he joined Jilin University. He is currently a professor with College of Electronic Science and Engineering, Jilin University. His current areas of interest include photonics, integrated optics, and optical fiber sensors.

Geyu Lu received the B.S. degree in electronic sciences in 1985 and the M.S. degree in 1988 from Jilin University in China and the Dr. Eng. degree in 1998 from Kyushu University in Japan. Now he is a professor of Jilin University, China. Presently, he is interested in the development of functional materials and chemical sensors.